Synthesis and Two-Photon-Excited Fluorescence of Benzothiazole-Based Compounds with Various π-Electron Donors

Du-Xia Cao,[a] Qi Fang,*[a] Dong Wang,[a] Zhi-Qiang Liu,[a] Gang Xue,[a] Gui-Bao Xu,[a] and Wen-Tao Yu[a]

Keywords: Fluorescence / Sulfur heterocycles / Wittig reactions

We have synthesized a series of new D–π–A compounds that feature various electron donors and a fixed benzothiazolyl unit as an electron acceptor. The crystal structure of compound **3** [*trans*,*trans*-2-{4-[(4-*N*-carbazolyl)styryl]styryl}-1,3-benzothiazole, **CSSB**] was determined. All these compounds show high fluorescence quantum yields and **3** in toluene gives the most intense blue emission around 450 nm with a quantum yield of Φ = 0.69. When excited at 800 nm by a Ti:sapphire femtosecond laser, these compounds exhibit strong two-photon-excited fluorescence (TPEF) in the blue-to-orange region. The measured TPEF cross-section of compound **2** [*trans*,*trans*-2-{4-[4-(*N*,*N*-diphenylamino)styryl]-styryl}-1,3-benzothiazole, **DPSSB**], for example, is about 6.1 times that of Coumarin 307. Photophysical data indicate that these compounds are polar in the ground state and have an enhanced polarity in the excited state, and that the electron donating ability of a dialkylamino group is much stronger than that of a diarylamino group.

Introduction

Two-photon-excited fluorescence (TPEF) is characterized by the unusual excitation manner of simultaneous absorption of two photons, each of which individually matches only half of the molecular energy level. Typically, as for the examples in this paper, blue TPEF can be excited by red light, i.e., the frequency of TPEF has been up-converted relative to that of the excitation light. Increasingly, two-photon absorption (TPA) and TPEF show several advantages over common linear absorption and single-photon excited fluorescence (SPEF) techniques, such as increased depth of penetration, reduced photodamage and greatly enhanced three-dimensional spatial resolution, which intrinsically originate from the quadratic dependence of TPA and TPEF on the intensity of the incident laser.[1,2] In recent years, new compounds with large TPA cross-sections or TPEF cross-sections have received much research interest and have shown promising applications in, for example, three-dimensional optical data storage,[3] optical power limiting,[4,5] two-photon-pumped frequency up-conversion lasing,[6,7] TPEF-based microscopy,[8] and photodynamic therapy.[9]

In the design of novel and useful TPA-based compounds for various applications, some figures of merit must be taken into consideration. Of crucial importance are a large TPA cross-section (σ), high SPEF and TPEF quantum yields (Φ and Φ′, respectively), and large TPEF cross-sections (which can be formulated as σΦ′). Photostability and proper response wavelengths also have to be taken into consideration. From the viewpoint of molecular engineering, structural features such as the π-conjugation style, the molecular planarity, and the donating and withdrawing abilities of the electron donor (D) and acceptor (A) all play an important role in increasing σ, Φ, and σΦ′. Most of the newly synthesized TPEF-active molecules can be classified as either asymmetrical D−π−A or symmetrical D−π−D/A−π−A types.[2,10−17]

By fixing a definite donor and π-bridge and then changing a series of different acceptors, Kannan et al. recognized that benzothiazolyl is an excellent acceptor that gives rise to a D−π−A type compound (**AF-240**, Scheme 1) that shows an optimized TPA cross-section when compared with the AF-X series of TPA compounds.[10] Kannan et al. also reported that the chemical, thermal, and photochemical stabilities of benzothiazolyl derivatives are much better than structurally similar compounds.[10] By fixing the benzothiazolyl unit as an optimized acceptor and then changing a series of different donors or π-bridges, the molecular structures may be further optimized for TPA and TPEF.

Based on these ideas, we recently synthesized a series of new D−π−A-type compounds, where D is a number of tertiary amino or thiophene groups, A is fixed as a benzothiazolyl unit and the π-bridge is extended to two conjugated styryl units. We believed that the skeleton of this π-bridge maintained basically planar, since planarity is commonly

[a] State Key Laboratory of Crystal Materials,
Shangdong University,
Shanda South Road 27, Jinan, 250100, China
Fax: (internat.) +86-531-8565403
E-mail: fangqi@icm.sdu.edu.cn

  DOI: 10.1002/ejoc.200300272

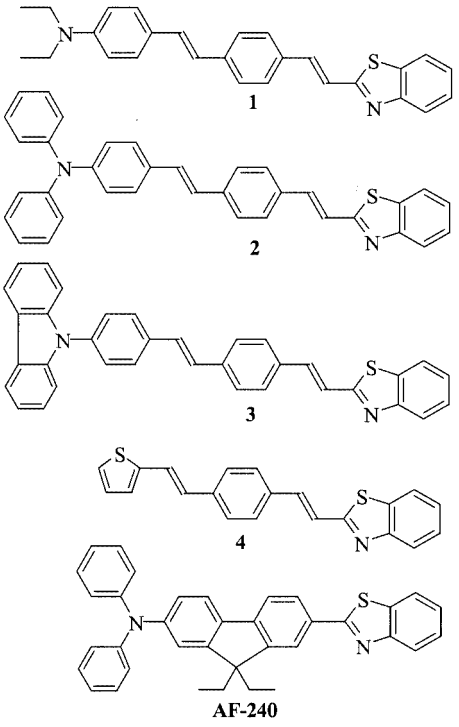

Scheme 1. Molecular structures of the compounds studied in this work and of **AF-240**[10]

regarded as a positive structural factor in enhancing the molecular TPA, SPEF, and TPEF properties.

As expected, these compounds possess high fluorescence quantum yields in the blue-to-orange region. Particularly, when excited by a tunable femtosecond laser at an excitation wavelength of 800 nm, they showed strong TPEF. In this paper, we report the detailed synthesis, structure and photophysical properties of these new compounds.

Results and Discussion

1. Synthesis

As outlined in Scheme 2, we synthesized the title compounds by cyclization, bromination, and subsequently a modified Wittig reaction. By a similar method described by Rose,[18] 2-aminothiophenol and 4-methylcinnamic acid were cyclized in phosphorus oxychloride to afford **5′** with high yield. To prepare the phosphonium salt for Wittig reaction, bromination is necessary, but the yield of bromination of **5′** to the product **6′** by using *N*-bromosuccinimide (NBS) is quite low (ca. 35%). This low yield may be because of the presence of an alkaline N atom on the benzothiazolyl unit. The phosphonium salt **7′** can be prepared conveniently from **6′** and one equivalent triphenylphosphane. Finally, the title compounds were obtained by Wittig reactions using **7′** and the aldehydes **1′**−**4′**. We stress that the Wittig reactions would produce mixtures of the *trans*- and *cis*-alkenes. The *trans*-configured object compounds possess higher chemical-, themal- and photo-stability and better fluorescence properties. To obtain pure *trans*-object compounds, all the crude products were treated with a trace amount of iodine in toluene, and the *trans*-configured ones were separated out by column chromatography on silica gel and purified by recrystallization from chloroform. All these new compounds were characterized by ^{1}H NMR, IR, and UV spectroscopy, MS spectrometry, and elemental analysis (the details are shown in the Exp. Sect.).

2. Structural Features of 3

There are two types of disorder: one that affects the C19 and C20 atoms in the π-bridge and the other that affects the C2 and C11 atoms in the carbazolyl unit (shown in Figure 1). The disorder of the π-bridge (C19, C20) is over two orientations and the major part (C19′, C20′) has an occupancy factor of 0.63. Other disorder pairs (C2 and C2′, C11 and C11′) have similar occupancy.

The molecular structure of **3** has been clearly characterized by inspecting the planarity of the carbazolyl and benzothiazolyl groups and several dihedral angles in the molecule. As shown in Figure 1, the dihedral angle between the carbazolyl plane (P1) and its neighboring phenyl plane (P2: C13 to C18) is 53.95°, while the dihedral angle between P2 and the central phenyl plane (P3: C21 to C26) is only

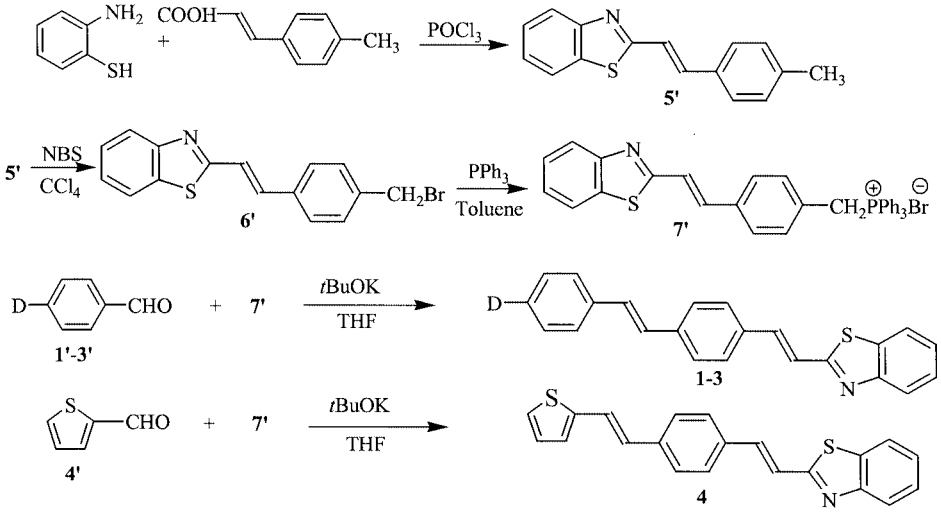

Scheme 2. Synthetic strategy for the preparation of the compounds (D = diethylamino, diphenylamino, carbozolyl)

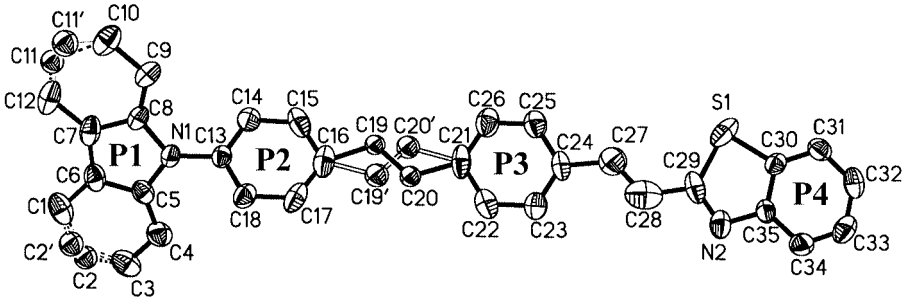

Figure 1. Molecular structure of **3**. Hydrogen atoms have been omitted for clarity

14.28°, and the dihedral angle between P3 and the terminal phenyl plane (P4: C30 to C35) is 7.91°. These data indicate that the benzothiazolyl acceptor is so highly conjugated with the π-bridge that it has become part of the whole π-delocalization system; the donor, however, which is seriously twisted with respect to the main molecular plane, does not conjugate well with the π-bridge. Thus, the co-planar benzothiazolyl unit can make good use of its electron accepting ability. A further survey of the π-bridge, which extends to the benzothiazolyl group, reveals that the dihedral angle between P2 and P4 (22.16°) is almost equal to the sum of that between P2 and P3 (14.28°) and that between P3 and P4 (7.91°), showing that the planar π-bridge has become gradually and slightly skewed. Although detailed X-ray structures of **1**, **2**, and **4** are not available, we believe that these benzothiazole-based title compounds probably have similar structures to that of **3** in that their conjugated π-bridges and benzothiazolyl groups are basically coplanar.

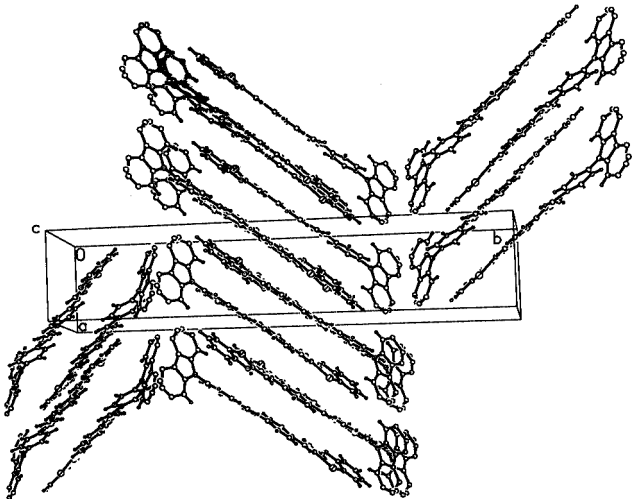

Figure 2. Packing diagram for **3** viewed along the *c* axis

Figure 2 shows the view along the *c* axis of the packing diagram of compound **3** in the crystal. The structures can be regarded as consisting of alternating (010) layers. The molecules in two adjacent layers are nearly perpendicular to each other, forming a herring-bone-like structure, and all of the carbazolyl groups are located between the adjacent layers. By viewing a certain molecular (010) layer, we observe that molecules of **3** form columns along the *a* axis and form sheets along the *c* axis, and that all the main molecular planes are parallel to each other with neighboring molecules in the *a* direction being arranged in a head-to-tail manner.

3. Linear Absorption and Single-Photon-Excited Fluorescence

The photo-physical properties of the title compounds in four kinds of solvent are listed in Table 1. Figure 3 displays the typical linear absorption and SPEF spectra of these compounds in THF. The positions of the fluorescence peaks of these compounds are independent of the excitation wavelength in the absorption region and the quantum yields are also basically independent of the excitation wavelength from 370 nm to 430 nm. Some notable spectral features can be summarized as follows.

3.1. The Spectral Sequence and the Ground-State Polarity

As shown in Table 1 and Figure 3, the main absorption and fluorescence peaks of **3** appear at relatively shorter wavelengths, those of **1** appear at much longer wavelengths, and those of **2** are located in between. Thus, the peak positions (with respect to wavelength) occur in a sequence **1** > **2** >> **3** (red-shift sequence).

This spectral sequence is maintained invariably in all of the solvents used. It may correlate with the sequence of electron-donating strengths of corresponding donors and, therefore, be in accord with their sequence of molecular polarities.

It is interesting to survey whether the lone electron pair of the amino group is delocalized and, if it is, how it is delocalized. As shown in the structure of **3**, the NC_3 core in the carbazolyl unit basically is planar, with the distance of the N atom to the C_3 plane being only 0.0181 Å (this distance can be defined as the pyramidalization of the NC_3 core). The NC_3 plane is co-planar with the carbazolyl plane rather than co-planar with the next phenyl plane (P2). The N−C bond lengths in the carbazolyl unit [N(1)−C(5): 1.405 (7) Å, N(1)−C(8): 1.386 (7) Å] are considerable shorter than the N(1)−C(13) length [1.410 (7) Å]. These structural features are quite common in all of the carbazolyl derivatives collected by the Cambridge Structural Database (CSD). Thus, the lone electron pair is highly delocalized and is mainly delocalized within the carbazolyl group (P1 plane).

Table 1. Photophysical data of the title compounds

	Solvents	λ_{max}(abs.) [nm][a]	λ_{max}(SPEF) [nm][a] [b]	$\Delta\tilde{\nu}$ [cm^{-1}]	$10^3 \times m$[c]	$\Delta\mu_{ge}$[d] [D]	Φ[a] [e]	t [ns]	λ_{max}(TPEF) [nm][f]	σ[g] [GM][h]	σ_e[i]
1 (**DESSB**)	toluene	428	528	4638			0.54	1.6	528	116	3.3
	THF	425	590	7018			0.35	2.3	590	206	3.8
	acetone	423	644	8306			0.13	1.9			
	CH_3CN	421	656	8738	13.78	24.5	0.11	2.0			
2 (**DPSSB**)	toluene	417	514	4601			0.61	1.3	515	190	6.1
	THF	412	552	6578			0.49	2.0	551	221	5.7
	acetone	408	606	8070			0.22	2.2			
	CH_3CN	406	614	8501	13.04	27.2	0.17	2.3			
3 (**CSSB**)	toluene	387	444, 460	3468, 4242			0.69	1.0	449, 472	99	3.6
	THF	384	486	5880			0.61	1.4	487	118	3.8
	acetone	381	516	7162			0.54	2.0			
	CH_3CN	380	526	7589	12.48	25.7	0.49	2.2			
4 (**TESB**)	toluene	388	438, 460	3046, 4360			0.45	0.9	443, 467	42	1.0
	THF	380	473	5611			0.41	1.0	474	65	1.4
	acetone	377	494	6525			0.33	1.0			
	CH_3CN	377	502	6840	10.58	19.4	0.29	1.0			

[a] Linear absorption and SPEF properties were measured at $c = 5.0 \cdot 10^{-6}$ M. [b] For **1** and **2**, the excitation wavelength was 420 nm; for **3** and **4**, it was 390 nm. [c] The slope of plots of $\Delta\tilde{\nu}$ versus Δf. [d] The change in dipole moment, derived from the Lippert−Mataga equation. [e] Determined using Coumarin 307 as a standard ($\Phi = 0.56$)[19] with the excitation at 400 nm. [f] TPEF maxima excited with an 800-nm laser at $c = 1.0 \cdot 10^{-4}$ M. [g] The TPA cross-sections were measured by comparing their TPEF with that of Coumarin 307. [h] 1 GM = 10^{-50} ($cm^4 \cdot s$)/photon. [i] The relative TPEF cross-sections assuming that of Coumarin 307 is equal to 1.

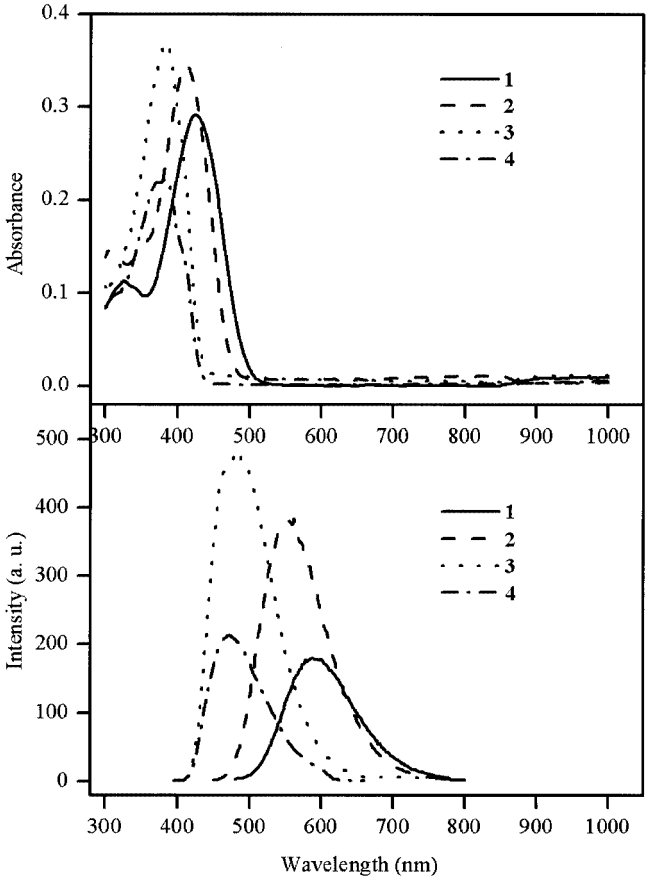

Figure 3. Linear absorption and single-photon-excited fluorescence in THF at $c = 5.0 \cdot 10^{-6}$ M

For all triphenylamino compounds collected in the CSD, the three phenyl rings are arranged in a propeller-like, noncoplanar fashion. As a statistical result, the pyramidalization of the NC_3 core in them is larger than that in carbazolyl derivatives. For example, the pyramidalization of NC_3 in (*E*)-4,4′-bis(diphenylamino) stilbene is 0.0436 Å and its three N−C bond lengths are very similar.[20] Thus, the lone electron pairs in triphenylamino compounds may be delocalized averagely over the three phenyl units. The NC_3 core in alkylamino compounds also tends to be planar and so the electron pair is also highly delocalized.[21] In contrast to the case of **3**, it must be delocalized mainly toward the acceptor in **1**.

Because of the delocalization of the lone pair of electrons to the diphenyl or carbazolyl (more significantly) units and the serious twist of the carbazolyl unit relative to the π-conjugated bridge, the electron-donating strength should be in the order diethylamino > diphenylamino >> carbazolyl (donating sequence). This sequence is supported by the corresponding ^{1}H NMR chemical shift data of the aldehyde protons in the precursor compounds: δ = 9.69, 9.78, and 10.01 ppm for **1**′, **2**′, and **3**′, respectively.

3.2. The Stokes Shifts and the Increased Excited-State Polarity

The solvatochromic effect for these compounds is enormous. For any one of these compounds, upon increasing the solvent polarity the absorption λ_{max} shows a small blue shift, the emission λ_{max} is remarkably red-shifted, and the quantum yields decrease. Thus, as shown in Table 1, the Stokes shifts $\Delta\tilde{\nu}$ of this series of compounds are all significantly large in various solvents and occur in the sequence **1** > **2** >> **3** (sequence of Stokes shift).

For polar compounds, the solvating interactions can be mainly attributed to the dipole−dipole interactions between

the solute and the solvent molecules. Increased polarity of a solvent and/or increased polarity of a solute will lead to greater lowering of the energy level. The bathochromic effect of SPEF above indicates that the dipole moment of these compounds should be much larger in the excited state than that in the ground state. In another words, the dipole moment in the ground state may be greatly enhanced in the excited state by the photoinduced charge transfer.

According to the Lippert−Mataga equation,[22] the Stokes shifts $\Delta\tilde{\nu}$ can be related to the difference in dipole moments ($\Delta\mu_{ge} = \mu_e - \mu_g$) between the ground and the excited states:

$$\Delta\bar{\nu} = \bar{\nu}_a - \bar{\nu}_f = 2\Delta\mu_{ge}^2\Delta f / hca^3 + \text{const} \quad (1)$$

with $\Delta f = [(\varepsilon - 1)/(2\varepsilon + 1)] - [(n^2 - 1)/(2n^2 + 1)]$

In this equation, a is the cavity radius of the molecule, Δf is the so-called orientation polarizability with ε and n being the dielectric constant and the refractive index, respectively, of the solvent.

By varying different solvents, the Stokes shifts $\Delta\tilde{\nu}$ show a fairly good linear relation with Δf (shown in Figure 4). Thus, the slope m of the fitted line of the $\Delta\tilde{\nu}$ vs. Δf data will give the term $2\Delta\mu_{ge}^2/hca^3$, which can serve as a convenient experimental measure of the dipole moment increase between the ground and excited states. The AM1 geometry optimization procedure gives the total surface area of a molecule and its equivalent a value was obtained by assuming the molecule to be a sphere having this surface area. In this way, the slope m and the resulting value of $\Delta\mu_{ge}$ were obtained and are listed in Table 1. Compound **1** has the largest m value and **2** has the largest value of $\Delta\mu_{ge}$ because of its largest a value. All $\Delta\mu_{ge}$ values are positive, suggesting a considerably increased dipole moment for the excited state.

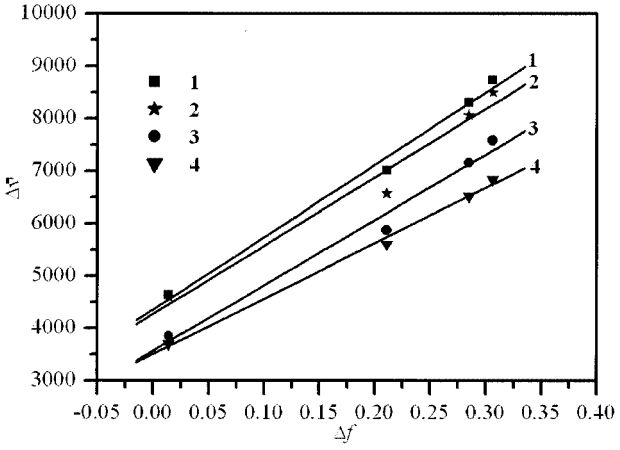

Figure 4. Stokes shift $\Delta\tilde{\nu}$ vs. orientation polarizability Δf of the solvents. (The scatter dots are the experimental data and the lines are the linearly fitted results.)

The structure type of **4** is quite different from that of the other three compounds. Because of the shorter conjugated chain, the absorption and fluorescence peaks in various solvents are blue-shifted relative to the other compounds, while the solvent-induced red-shift behavior is the same.

Benzothiazolyl seems not to be so well known as are other electron acceptors. Our photophysical data indicate that the benzothiazolyl unit behaves as an acceptor in the excited state. The benzothiazolyl group is also a conjugated delocalization system, as can be deduced by the X-ray structure of **3**. The polarity, π-delocalization, and photoinduced charge-transfer characteristics of a molecular system are basic structural factors in various branches of molecular nonlinear optics, including TPA- and TPEF-related photophysics.

Among these compounds, **3** stands out as having the best SPEF qualities: high quantum yields, a short blue-green emission wavelength, high chemical and photochemical stability, and easily crystallized, i.e., easy to purify.

4. Two-Photon-Excited Fluorescence Properties

The setup for TPEF measurement is depicted in Figure 5. A laser beam from a Ti:sapphire mode-locked femtosecond laser (Coherent, Mira 900-D) was used as a pump source and a streak camera (Hamamatsu, C5680) in conjunction with an imaging spectrograph (Hamamatsu, C5094) was used as a recorder. TPEF was detected at a direction perpendicular to the pump beam. To minimize the effects of re-absorption, the excitation beam was focused as close as possible to the wall of the quartz cell, which faced the slit of the imaging spectrograph.

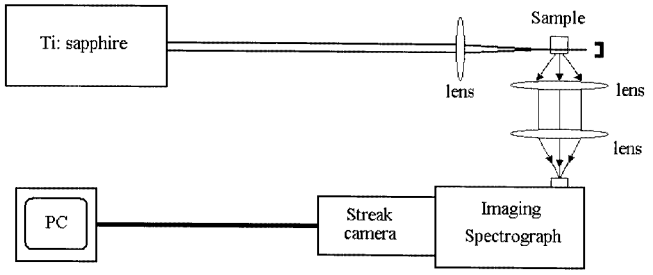

Figure 5. Experimental setup for TPEF measurement

As shown in Figure 3, there is no detectable linear absorption from 550 to 1000 nm and, therefore, there should be no such molecular energy level corresponding to this wavelength range. Thus, upon excitation from 710 nm to 900 nm, there should be no possibility of producing single-photon-induced up-conversion fluorescence and no such intermediate step allowing a cascading excitation, such as is the case for some inorganic, frequency up-conversion materials. The only reasonable excitation mechanism is a two-photon mechanism, i.e., simultaneous absorption of two photons by each molecule.

As shown in Figure 6, the TPEF intensity of compound **2** shows a quadratic dependence on the input power when the input laser power is below 0.13 W, which suggests the two-photon excitation mechanism. Above 0.13 W, however, TPEF intensity increases slowly and the quadratic rule is obviously not in effect, implying some uncertain photophysical processes, which cause the fluorescence saturation, are in effect.

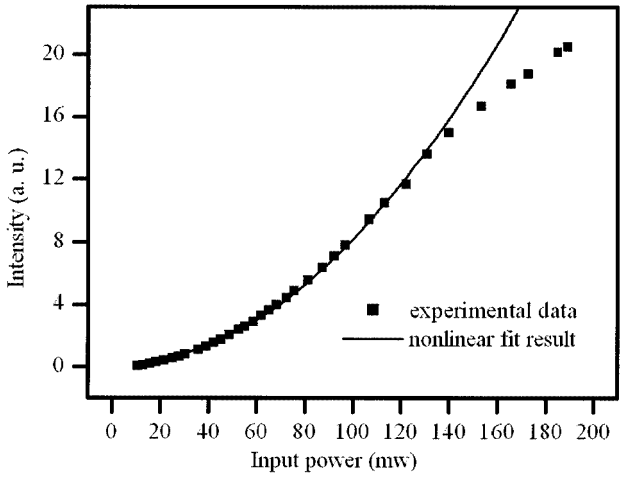

Figure 6. The output fluorescence intensity vs. the input power for **2** in THF with $c = 1.0 \cdot 10^{-3}$ M

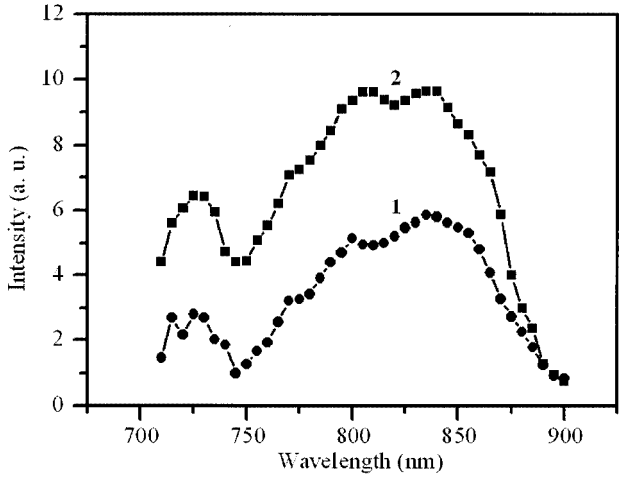

Figure 7. Two-photon excitation (TPE) spectra of **1** and **2** in THF with $c = 1.0 \cdot 10^{-3}$ M

Detailed experiments reveal that from 710 to 900 nm the peak positions in the TPEF spectra of these compounds are independent of the excitation wavelengths, but the emission intensities of TPEF are dependent over that range. By tuning the pump wavelengths incrementally from 710 to 900 nm while keeping the input power fixed and then recording TPEF intensity, two-photon excitation (TPE) spectra were obtained; the TPE spectra of **1** and **2** are shown in Figure 7. The spectra display two excitation peaks, and this feature is quite similar to that observed in the linear absorption spectra, except that the wavelengths are roughly doubled. The optimal excitation wavelengths for **1** and **2** are ca. 820 nm. The TPE peak of **2** is essentially twice that of linear absorption maximum (412 nm), but the TPE peak for **1** is at an energy slightly higher than twice that of the corresponding linear absorption maximum (425 nm).

The TPEF spectra of all these compounds, shown in Figure 8, were taken when they were excited at 800 nm in THF. The TPEF of Coumarin 307 was measured as a standard under the same experimental conditions. All of our compounds show much stronger frequency up-converted fluorescence than that of Coumarin 307.

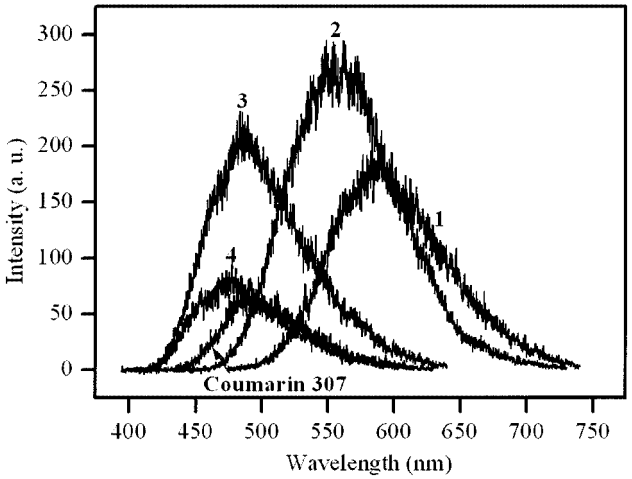

Figure 8. Two-photon-excited fluorescence spectra of the compounds in THF and of Coumarin 307 in MeOH at $c = 1.0 \cdot 10^{-4}$ M

The TPEF characteristics of the compounds are also affected by their molecular environments. Just like the effect of solvent on SPEF, the peak position of TPEF is red-shifted with increasing the solvent polarity from toluene to THF. The TPEF peak positions of **3** and **4** in toluene show a small red-shift relative to their corresponding SPEF peaks. This red-shift might originate from the re-absorption of the fluorescence within the concentrated solution. Taking **3** in toluene as an example, the shorter-wavelength side of the SPEF peak and the longer-wavelength side of the linear absorption band are overlapped to some extent (see Figure 9). For all the compounds in THF, and **1** and **2** in toluene, the Stokes shifts are large enough that the emission and absorption bands hardly overlap and, thus, their TPEF peaks have no obvious shift. For the Coumarin 307 solution in MeOH, the position of the TPEF peak (490 nm) is the same as that of the SPEF peak.

Based on the similarities of the SPEF and TPEF of these benzothiazole-based compounds, we recognize that the pri-

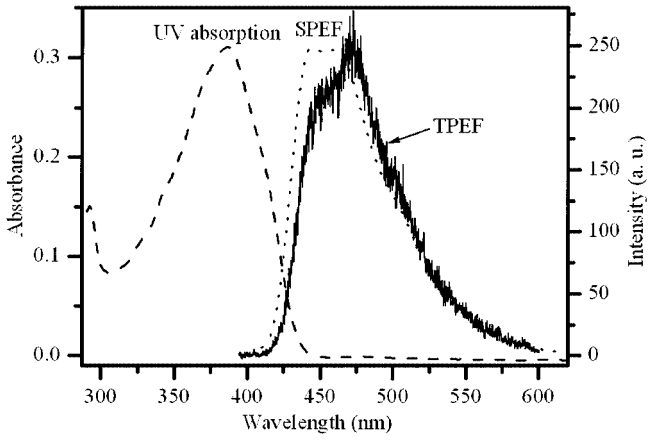

Figure 9. The UV absorption and single-photon-excited fluorescence (SPEF) spectra ($c = 5.0 \cdot 10^{-6}$ M) and the two-photon-excited fluorescence (TPEF) spectrum ($c = 1.0 \cdot 10^{-4}$ M) of **3** in toluene

mary excited states obtained by single-photon absorption and two-photon absorption may be different because of the different parity selection rules, but they are likely to relax quickly to the same fluorescence emission states.

5. TPA and TPEF Cross-Sections

The TPA and TPEF cross-sections (σ and σ_e, respectively) are basic parameters to evaluate a material's TPA and TPEF properties. From TPEF intensity data, σ_e and σ can be evaluated by using Equations (2) and (3),[23,24] where *r* stands for the reference compound, *n* for the refractive index, and *F* for the integral fluorescence intensity.

$$\sigma_e = \sigma_{e,r} \frac{F n_r}{F_r n} \quad (2)$$

$$\sigma = \frac{\sigma_e}{\Phi'} \quad (3)$$

We obtained the relative TPEF cross-sections σ_e of these compounds by comparing their TPEF to that of Coumarin 307 under exactly the same experimental conditions, and by specifying that the value for Coumarin 307 be equal to 1. As listed in Table 1, compound **2** shows the largest TPEF cross-section, which is 6.1 times that of Coumarin 307, at the 800 nm excitation.

The TPEF cross-section σ_e is supposed to be linearly dependent on the TPA cross-section (σ) with the TPEF quantum yield Φ' as the coefficient.[24] In most reports, the SPEF quantum yield Φ has been adopted instead of Φ', because Φ' is difficult to measure. By referencing the TPEF cross-section of Coumarin 307 to be 19 GM (1 GM = 10^{-50} $cm^4 \cdot s/photon$),[23] the TPA cross-sections of the title compounds were obtained (Table 1); they are a few times larger than that of the Coumarin 307 reference. Compound **2** in THF shows the largest TPA cross-section (221 GM). Compound **4** shows the smallest TPA and TPEF cross-sections, which may be because of its shorter conjugation system. Although compound **3** possesses the best SPEF qualities, compound **2** exhibits the best TPEF properties by having the largest TPA and TPEF cross-sections at the two-photon excitation wavelength (800 nm). By comparison with compound **1**, the much better SPEF and TPEF properties of **2** might result from its propeller-shaped diphenylamino group, which (1) can properly partition the lone electron pair and stabilize the reduced positive charge and (2) can help to form and stabilize the fluorescent state having charge-transfer character. By comparison with compound **3**, which also possesses an aromatic arylamino-substituted donor, the superior TPEF properties of **2** might be attributable to (1) the greater electron donating ability of a diphenylamino group relative to that of a carbazolyl group and (2) the TPEF excitation wavelength (800 nm) for **3** not being short enough, considering the λ_{max} (384 nm in THF) of the absorption spectra of **3**.

Conclusion

We have synthesized a series of new benzothiazole-based compounds incorporating various electron donor groups. The photophysical data of these compounds indicate that benzothiazolyl is a true electron acceptor in its excited state. All these compounds show very strong two-photon-excited, frequency up-converted fluorescence ranging from blue to orange, with the TPA cross-sections on the order of 10^2 GM. By fixing the benzothiazolyl acceptor and then testing a series of different donors, we found that although the diethylamino group provides the strongest donating properties, the most suitable donor for TPA and TPEF may be the diphenylamino group.

Experimental Section

General Remarks: Nuclear magnetic resonance spectra were recorded on a Bruker AV 600 spectrometer. Infrared spectra were recorded on a Nicolet 20SX FT-IR spectrophotometer. Mass spectra were obtained on an Agilent 5973N MSD spectrometer. The melting points were measured on a Mettler−Toledo DSC822e Differential Scanning Calorimeter at a heating rate of 20 °C·min^{-1} under a nitrogen atmosphere. Elemental analyses were carried out on a PE 2400 autoanalyzer. 2-Aminothiophenol, 4-methylcinnamic acid, and 2-thiophenecarbaldehyde (**4′**) were obtained from Acros Ltd. 4-(Diethylamino)benzaldehyde (**1′**) and 4-(*N*-carbazolyl)benzaldehyde (**3′**) were synthesized according to a literature procedure.[25] 4-(Diphenylamino)benzaldehyde (**2′**) was prepared by a standard Vilsmeier reaction. All the solvents used for absorption and fluorescence measurements were HPLC grade. Linear absorption spectra of dilute solutions ($c = 5.0 \cdot 10^{-6}$ M) were recorded on a Hitachi U-3500 UV/Vis-IR spectrophotometer using a quartz cuvette having 1-cm path length. Steady-state fluorescence spectra and fluorescence decay curves were measured on an Edinburgh FLS920 fluorescence spectrometer equipped with a 450-W Xe lamp and a time-correlated single-photon counting (TCSPC) card. All the fluorescence spectra were corrected. The SPEF quantum yields Φ were measured by using a standard method with excitation at 400 nm under the same experimental conditions for all compounds.[26] Coumarin 307 dissolved in ethanol, at the same concentration as the other samples, was used as the standard.[19] Lifetime values were obtained by reconvolution fit analysis of the decay profiles with the aid of F900 analysis software. The fitting results were judged by their values of "reduced chi-squared". Two-photon-excitation (TPE) and TPEF spectra (excited by 800 nm laser) were measured using a Mira 900-D Ti:sapphire femtosecond laser with a pulse width of 200 fs and a repetition rate of 76 MHz.

2-[2-(4-Methylphenyl)ethenyl]-1,3-benzothiazole (5′): 4-Methylcinnamic acid (8.1 g, 0.05 mol) and 2-aminothiophenol (5.4 mL, 6.3 g, 0.05 mol) were suspended in phosphorus oxychloride (ca. 60 mL) and then the mixture was heated at 100 °C under nitrogen for 5 h. After the mixture had cooled to room temperature, it was carefully and slowly poured into a beaker of stirring distilled water (200 mL). The pH was adjusted to 7.0 by addition of sodium hydroxide pellets. The crude product was extracted into dichloromethane and washed twice with distilled water. The organic solvent was removed using a rotary evaporator. The separated precipitate was repeatedly recrystallized from ethanol to give colorless platelet crystals (10.0 g, 80%). ^{1}H NMR ($CDCl_3$): δ = 2.38 (s, 3 H), 7.10−7.61 (m, 8 H), 7.75−8.06 (m, 2 H) ppm.

2-{2-[4-(Bromomethyl)phenyl]ethenyl}-1,3-benzothiazole (6′): Compound **5′** (6.3 g, 0.025 mol) was dissolved in freshly distilled tetrachloromethane (200 mL) and then *N*-bromosuccinimide (4.5 g,

0.025 mol) and a small amount of benzoyl peroxide were added together. The mixture was heated under reflux for 8 h. After cooling to room temperature, the precipitate was filtered off and the filtrate was purified by column chromatography on silica gel using chloroform/petroleum ether (1:9) as eluent. A colorless powder was obtained (2.9 g, 35%). ^{1}H NMR ($CDCl_3$): δ = 4.50 (s, 2 H), 7.21−7.62 (m, 8 H), 7.76−8.06 (m, 2 H) ppm.

{4-[2-(1,3-Benzothiazole-2-yl)ethenyl]benzyl}triphenylphosphonium Bromide (7′): A mixture of **6′** (4.0 g, 0.012 mol) and triphenylphosphane (3.2 g, 0.012 mol) in freshly distilled toluene (200 mL) was heated under reflux for 5 h. The mixture was then placed in a refrigerator overnight and then the crude precipitate was filtered off and washed with ethanol. A yellow powder (5.7 g, 80%) was obtained and used directly in the next step without further purification.

***trans*,*trans*-2-{4-[4-(*N*,*N*-Diethylamino)styryl]styryl}-1,3-benzothiazole (1, DESSB):** A mixture of **7′** (2.5 g, 0.004 mol) and **1′** (0.71 g, 0.004 mol) was suspended in freshly distilled THF (40 mL) and then potassium *tert*-butoxide (0.7 g, 0.006 mol) in *tert*-butyl alcohol (60 mL) was added dropwise under nitrogen with stirring in an ice-bath. The mixture was continuously stirred at room temperature for further 20 h. The mixture was poured into a beaker containing distilled water (200 mL) and the pH value of the mixture was adjusted to 7.0 by addition of dilute hydrochloric acid. This mixture was extracted with dichloromethane, the organic phases were washed twice with distilled water, and then the organic solvent was removed using a rotary evaporator. To isomerize the crude material to the *trans*-configured object compound, the residue was dissolved in toluene (ca. 50 mL) containing a trace amount of iodine and then the mixture was heated under reflux for further 4 h. The solvent was evaporated, the residue was purified by column chromatography on silica gel using chloroform/petroleum ether (1:1) as eluent, and the product was then recrystallized from chloroform to yield a red powder (0.66 g, 40%). M.p. 227−230 °C, ^{1}H NMR (600 MHz, $CDCl_3$): δ = 1.21 (t, *J* = 7.0 Hz, 6 H), 3.41 (q, *J* = 7.0 Hz, 4 H), 6.69 (d, *J* = 8.6 Hz, 2 H), 6.91 (d, $J_{(E)}$ = 16.2 Hz, 1 H), 7.13 (d, $J_{(E)}$ = 16.2 Hz, 1 H), 7.37−7.43 (m, 4 H), 7.47−7.57 (m, 6 H), 7.88 (d, *J* = 8.0 Hz, 1 H), 8.01 (d, *J* = 8.1 Hz, 1 H) ppm. MS: *m*/*z* (%) = 410 (100) [M^+], 395 (89) [$M - CH_3$]$^+$. UV/Vis (THF): λ_{max} (ε) = 425 nm ($5.8\cdot10^4$). IR (KBr): $\tilde{\nu}$ = 2969 (w), 1585 (s), 1519 (s), 1478 (m), 1402(m), 1357 (m), 1266 (s), 1186 (s), 1152 (s), 961 (s), 818 (s), 757 (s), 731 (m) cm^{-1}. $C_{27}H_{26}N_2S$ (410.6): calcd. C 78.99, H 6.38, N 6.82, S 7.81; found C 78.68, H 6.31, N 6.65, S 7.69.

***trans*,*trans*-2-{4-[4-(*N*,*N*-Diphenylamino)styryl]styryl}-1,3-benzothiazole (2, DPSSB):** By reaction of **2′** and **7′**, **DPSSB** was prepared as a yellow powder (0.85 g, 42%) following a method similar to that described above. M.p. 277−278 °C. ^{1}H NMR (600 MHz, $CDCl_3$): δ = 7.02 (d, $J_{(E)}$ = 16.3 Hz, 1 H), 7.05−7.08 (m, 4 H), 7.13−7.16 (m, 5 H), 7.28−7.30 (m, 4 H), 7.41−7.43 (m, 3 H), 7.45 (d, $J_{(E)}$ = 16.1 Hz, 1 H), 7.50−7.60 (m, 6 H), 7.89 (d, *J* = 7.9 Hz, 1 H), 8.03 (d, *J* = 8.1 Hz, 1 H) ppm. MS: *m*/*z* (%) = 506 (100) [M^+], 253 (24) [$M]^{2+}$. UV/Vis (THF): λ_{max} (ε) = 412 nm ($6.9\cdot10^4$). IR (KBr): $\tilde{\nu}$ = 3026 (w), 1588 (s), 1512 (m), 1489 (s), 1331 (m), 1280 (s), 1176 (m), 1107 (w), 961 (s), 826 (m), 755 (s), 729 (m), 695 (s) cm^{-1}. $C_{35}H_{26}N_2S$ (506.7): calcd. C 82.97, H 5.17, N 5.53, S 6.33; found C 82.39, H 5.07, N 5.31, S 6.49.

***trans*,*trans*-2-{4-[4-(*N*-Carbazolyl)styryl]styryl}-1,3-benzothiazole (3, CSSB):** By reaction of **3′** and **7′**, yellow-green microcrystals of **3** (0.91 g, 45%) were obtained following a procedure similar to that described above. Platelet crystals, which were suitable for X-ray crystallography, were obtained by recrystallization from chloroform. M.p. 296−297 °C. ^{1}H NMR (600 MHz, $CDCl_3$): δ = 7.26 (d, $J_{(E)}$ = 16.6 Hz, 1 H), 7.31−7.33 (m, 3 H), 7.41−7.51 (m, 7 H), 7.59 (d, $J_{(E)}$ = 16.7 Hz, 1 H), 7.61−7.64 (m, 6 H), 7.78 (d, *J* = 8.3 Hz, 2 H), 7.90 (d, *J* = 7.8 Hz, 1 H), 8.04 (d, *J* = 8.0 Hz, 1 H), 8.17 (d, *J* = 7.8 Hz, 2 H) ppm. MS: *m*/*z* (%) = 504 (100) [M^+], 252 (51) [$M]^{2+}$. UV/Vis (THF): λ_{max} (ε) = 384 nm ($7.4\cdot10^4$). IR (KBr): $\tilde{\nu}$ = 1593 (m), 1513 (s), 1477 (m), 1450 (s), 1334 (m), 1312 (m), 1231 (s), 1169 (w), 1103 (m), 955 (s), 824 (m), 750 (s), 724 (s) cm^{-1}. $C_{35}H_{24}N_2S$ (504.7): calcd. C 83.30, H 4.79, N 5.55, S 6.35; found C 83.04, H 4.81, N 5.50, S 6.31.

***trans*,*trans*-2-{4-[2-(Thiophen-2-yl)ethenyl]styryl}-1,3-benzothiazole (4, TESB):** By reaction of **4′** and **7′**, a yellow-green powder (0.53 g, 38%) was obtained. M.p. 240−241 °C, ^{1}H NMR (600 MHz, $CDCl_3$): δ = 6.95 (d, $J_{(E)}$ = 16.1 Hz, 1 H), 7.04 (m, 1 H), 7.13 (d, *J* = 3.3 Hz, 1 H), 7.25 (d, *J* = 5.0 Hz, 1 H), 7.32 (d, $J_{(E)}$ = 16.0 Hz, 1 H), 7.40 (t, *J* = 7.3 Hz, 1 H), 7.44 (d, $J_{(E)}$ = 16.1 Hz, 1 H), 7.49−7.60 (m, 6 H), 7.89 (d, *J* = 7.9 Hz, 1 H), 8.03 (d, *J* = 8.1 Hz, 1 H) ppm. MS: *m*/*z* (%) = 344 (100) [M^+]. UV/Vis (THF): λ_{max} (ε) = 380 nm ($4.4\cdot10^4$). IR (KBr): $\tilde{\nu}$ = 1619 (m), 1591 (m), 1477 (m), 1431 (m), 1412 (m), 1312 (m), 1231 (m), 1192 (m), 956 (s), 864 (m), 821 (s), 754 (s), 728 (s), 697 (s), 666 (m) cm^{-1}. $C_{21}H_{15}NS_2$ (345.5): calcd. C 73.01, H 4.38, N 4.05, S 18.56; found C 72.69, H 4.29, N 4.13, S 18.44.

X-ray Crystallographic Study of 3 (CSSB): X-Ray diffraction data of a yellow-green single crystal of **3** (0.45 × 0.42 × 0.08 mm) were collected on a Bruker P4 four-circle diffractometer using Mo-K_α radiation. Of 5781 collected reflections ($4.04 \le 2\theta \le 49.98$), 4569 reflections were independent (R_{int} = 0.0340). The structure was resolved using the SHELXTL-97 program by a direct method and refined by a full-matrix least-squares method on F^2. The crystal belongs to the monoclinic system, $P2_1/c$ space group, with formula $C_{35}H_{24}N_2S$ and molecular weight 504.62; *T* = 293(2) K, *a* = 8.0149(9), *b* = 40.378(4), *c* = 8.0607(12) Å, β = 97.480(10)°, *V* = 2586.4(5) Å^3, *Z* = 4, $d_{calcd.}$ = 1.306 Mg/m^3, μ = 0.153 mm^{-1}, *F*(000) = 1072, R_1 = 0.1005, wR_2 = 0.2586 [$I > 2\sigma(I)$].

CCDC-191317 contains the supplementary crystallographic data for this paper. These data can be obtained free of charge at www.ccdc.cam.ac.uk/conts/retrieving.html [or from the Cambridge Crystallographic Data Centre, 12, Union Road, Cambridge CB2 1EZ, UK; fax: (internat.) +44−1223/336-033; E-mail: deposit@ccdc.cam.ac.uk].

Acknowledgments

This work was supported by the National Nature Science Foundation of China (No. 20172034), the Foundation for University Key Teachers by the Ministry of Education, and by a grant from the State Key Program of China.

[1] J. D. Bhawalkar, G. S. He, P. N. Prasad, *Rep. Prog. Phys.* **1996**, *59*, 1041−1070.
[2] M. Albota, D. Beljonne, J.-L. Brédas, J. E. Ehrlich, J.-Y. Fu, A. A. Heikal, S. E. Hess, T. Kogej, M. D. Levin, S. R. Marder, D. McCord-Maughon, J. W. Perry, H. Röckel, M. Rumi, G. Subramaniam, W. W. Webb, X.-L. Wu, C. Xu, *Science* **1998**, *281*, 1653−1656.
[3] D. A. Parthenopoulos, P. M. Rentzepis, *Science* **1989**, *245*, 843−845.
[4] G. S. He, J. D. Bhawalkar, C. F. Zhao, P. N. Prasad, *Appl. Phys. Lett.* **1995**, *67*, 2433−2435.
[5] J. E. Ehrlich, X. L. Wu, I.-Y. S. Lee, Z.-Y. Hu, H. Röckel, S. R. Marder, J. W. Perry, *Opt. Lett.* **1997**, *22*, 1843−1845.

[6] G. S. He, C. F. Zhao, J. D. Bhawalkar, P. N. Prasad, *Appl. Phys. Lett.* **1995**, *67*, 3703−3705.
[7] Y. Ren, Q. Fang, W. T. Yu, H. Lei, Y. P. Tian, M. H. Jiang, Q. C. Yang, T. C. W. Mak, *J. Mater. Chem.* **2000**, *10*, 2025−2030.
[8] W. Denk, J. H. Strickler, W. W. Webb, *Science* **1990**, *248*, 73−76.
[9] H. Stiel, K. Teuchner, A. Paul, W. Freyer, D. Leupold, *J. Photochem. Photobiol. A: Chem.* **1994**, *80*, 289−298.
[10] R. Kannan, G. S. He, L. X. Yuan, F. Xu, P. N. Prasad, A. G. Dombroskie, B. A. Reinhardt, J. W. Baur, R. A. Vaia, L.-S. Tan, *Chem. Mater.* **2001**, *13*, 1896−1904.
[11] M. Rumi, J. E. Ehrlich, A. A. Heikal, J. W. Perry, S. Barlow, Z. Hu, D. McCord-Maughon, T. C. Parker, H. Röckel, S. Thayumanavan, S. R. Marder, D. Beljonne, J.-L. Brédas, *J. Am. Chem. Soc.* **2000**, *122*, 9500−9510.
[12] O.-K. Kim, K.-S. Lee, H. Y. Woo, K.-S. Kim, G. S. He, J. Swiatkiewicz, P. N. Prasad, *Chem. Mater.* **2000**, *12*, 284−286.
[13] L. Ventelon, L. Moreaux, J. Mertz, M. Blanchard-Desce, *Chem. Commun.* **1999**, 2055−2056.
[14] B. A. Reinhardt, L. L. Brott, S. J. Clarson, A. G. Dillard, J. C. Bhatt, R. Kannan, L. X. Yuan, G. S. He, P. N. Prasad, *Chem. Mater.* **1998**, *10*, 1863−1874.
[15] L. Ventelon, S. Charier, L. Moreaux, J. Mertz, M. Blanchard-Desce, *Angew. Chem. Int. Ed.* **2001**, *40*, 2098−2101.
[16] B. R. Cho, K. H. Son, S. H. Lee, Y.-S. Song, Y.-K. Lee, S.-J. Jeon, J. H. Choi, H. Lee, M. Cho, *J. Am. Chem. Soc.* **2001**, *123*, 10039−10045.
[17] Z. Q. Liu, Q. Fang, D. Wang, G. Xue, W. T. Yu, Z. S. Shao, M. H. Jiang, *Chem. Commun.* **2002**, 2900−2901.
[18] U. Rose, *J. Heterocyclic Chem.* **1992**, *29*, 551−557.
[19] G. A. Reynolds, K. H. Drexhage, *Opt. Commun.* **1975**, *13*, 222−225.
[20] X. M. Wang, D. Wang, G. Y. Zhou, W. T. Yu, Y. F. Zhou, Q. Fang, M. H. Jiang, *J. Mater. Chem.* **2001**, *11*, 1600−1605.
[21] Z. Q. Liu, Q. Fang, W. T. Yu, G. Xue, D. X. Cao, D. Wang, G. M. Xia, M. H. Jiang, *Chin. Chem. Lett.* **2002**, *13*, 997−1000.
[22] J. R. Lakowicz, *Principles of Fluorescence Spectroscopy*, Plenum Press, New York, **1983**, p. 190.
[23] C. Xu, W. W. Webb, *J. Opt. Soc. Am. B* **1996**, *13*, 481−491.
[24] M. A. Albota, C. Xu, W. W. Webb, *Appl. Opt.* **1998**, *37*, 7352−7356.
[25] C. F. Zhao, C.-K. Park, P. N. Prasad, Y. Zhang, S. Ghosal, R. Burzynski, *Chem. Mater.* **1995**, *7*, 1237−1242.
[26] J. N. Demas, G. A. Crosby, *J. Phys. Chem.* **1971**, *75*, 991−1024.
Received May 7, 2003

